NASA Technical Memorandum 112861

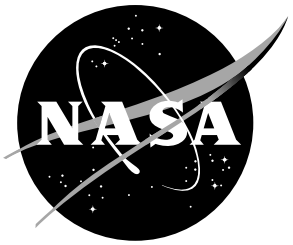

CFL3D: Its History and Some Recent Applications

Christopher L. Rumsey, Robert T. Biedron, and James L. Thomas
Langley Research Center, Hampton, Virginia

May 1997

National Aeronautics and
Space Administration
Langley Research Center
Hampton, Virginia 23681-0001

CFL3D: Its History and Some Recent Applications

Christopher L. Rumsey, Robert T. Biedron, and James L. Thomas
Mail Stop 128, NASA Langley Research Center, Hampton Virginia 23681

e-mail: c.l.rumsey@larc.nasa.gov

Presented at the "Godunov's Method for Gas Dynamics: Current Applications and Future Developments" Symposium, University of Michigan, May 1-2, 1997

History

The CFL3D (Computational Fluids Laboratory - 3D) computer code is a result of the close working relationship between computational fluid dynamicists at the NASA Langley Research Center and visiting scientists to the Institute for Computer Applications in Science and Engineering (ICASE) at the same location. In the early 1980's, computational fluid dynamics (CFD) was still an emerging field. By bringing together many of the leading scientists in numerical methods to work with each other, NASA and ICASE enabled the crystallization of many new ideas and methods for CFD.

The initial spark for the CFL3D code was the application of the flux-vector splitting (FVS) monotone upstream-centered scheme for conservation laws (MUSCL) idea of van Leer[1,2] to an implicit finite-volume code for the solution of the three-dimensional (3d) compressible Euler equations. Many of van Leer's ideas were inspired by the pioneering work of Godunov,[3] who considered the fluid to be divided into slabs and determined the interaction of these slabs at their interface. The team of Thomas, Anderson, Walters, and van Leer[4,5] explored several implicit solution strategies using FVS, particularly with regard to application on recently-developed vector-processor computers. Also, FVS was compared with other flux-splitting techniques, and various types of flux limiters were explored for transonic airfoil applications. The code was quickly extended to solve the 3d thin-layer Navier-Stokes equations.[6,7,8] Initial applications were made on leading-edge vortex flows, for which the viscous terms are necessary to capture the secondary flow features. At about this same time, research was initiated into applying multigrid methods to the implicit algorithm.[9] The three-factor approximate factorization (AF) strategy was settled upon as the best choice for a wide range of applications, due to its better smoothing rate and more complete vectorization than other strategies. It was determined that the conditional stability of three-factor AF is not a penalty since large time steps are generally not necessary for a multigrid smoothing algorithm. The multigrid algorithm with FVS and a fixed W-cycle cycling strategy was employed to solve the thin-layer Navier-Stokes equations over a delta wing in Thomas et al.[10]

In the mid-1980's, the flux-difference splitting (FDS) approximate Riemann solver of Roe,[11] also a derivative of Godunov's[3] work, was recognized as an important advance for upwind CFD methods. In van Leer et al,[12] the importance of including (in the numerical flux formula for the convective terms) information about all different waves by which neighboring cells interact was

discussed in relation to the Navier-Stokes equations. Flux functions based on the full Riemann solution, such as FDS, accurately represent both grid-aligned shocks and boundary layers. Other methods, including FVS (which ignores entropy and shear waves), are inferior in either shock and/or boundary layer rendition on all but the finest grids. Therefore, FDS was incorporated into the CFL3D code, and most subsequent Navier-Stokes applications employed it. For the left-hand side implicit operator, the spatial factors for FDS were approximated with a diagonal inversion plus a spectral radius scaling for the viscous terms, significantly increasing the speed of the code.[13] Vatsa et al[13] also drew a link between the natural dissipation inherent in FDS and the artificial dissipation employed in central-difference methods.

Although the laminar Navier-Stokes equations were solved for many vortex-dominated and low Reynolds number flows,[7,8,10,14] including hypersonic flows,[15] it was realized that the Reynolds-averaged Navier-Stokes equations (with the inclusion of a turbulence model) are necessary to adequately model the physics of most high Reynolds number aerodynamic flows of interest. The Baldwin-Lomax algebraic eddy viscosity turbulence model was the first incorporated into CFL3D,[13,16,17] with other more advanced one- and two-equation linear and nonlinear field-equation models to follow later.[18,19]

In the mid 1980's, research with CFL3D was also initiated toward solving the Euler and Navier-Stokes equations time-accurately, both for stationary bodies with inherently unsteady flow[20,21,22] as well as for unsteady flow over bodies in motion.[23,24,25] The time-advancement algorithm in the code has continued to evolve since that time, incorporating subiterations to reduce linearization and factorization errors, as well as employing a pseudo-time-stepping algorithm with multigrid to allow the use of more physically-relevant time steps for time-accurate turbulent flow computations.[26]

Beginning in the late 1980's, the CFL3D code's capabilities to solve flows over complex configurations were developed through the use of various grid-zone-connection strategies. Beside simple one-to-one connectivity, Thomas et al[16] introduced the patched-grid connection capability into the code with further enhancements and generalization made later,[27] including application to sliding patched-zone interfaces.[28] Overset grid capability was also included,[29] as was an embedded grid capability in order to employ finer mesh density in desired regions of interest such as a delta wing vortex core.[30]

CFL3D is currently used by well over one hundred researchers in twenty-two different companies in industry, thirteen universities, as well as at NASA and in the military. It owes much of its success to its strong foundation in the upwind methods that arose from Godunov's original ideas.

Recent Applications

CFL3D has been applied to flow regimes ranging from low-subsonic to hypersonic. Configurations have ranged from flat plates to complete aircraft with control surfaces. Below we present a few of the recent applications carried out by NASA-Langley researchers.

Partial-Span Flap

Figure 1 shows the results of an analysis of a rectangular wing with a 58% span flap.[31] Shown

in the figure is a representative view of the grid, which makes use of the generalized grid-patching capability of the code. Also shown are computed total pressure contours on the surface and streamline traces following the roll-up of the flap-edge and wing-tip vortices. Comparison to wind-tunnel pressure data indicate that flow over both the flap and the wing are accurately computed.

F/A-18 Forebody Control Strake

At high angles of attack, traditional yaw-control devices such as the rudder lose effectiveness due to immersion in the low-speed wake of the wing. The forebody-strake concept was developed in order to provide control effectiveness at very large angles of attack. Figure 2 shows two results from CFL3D computations that were performed to help validate the forebody-strake concept. In the top part of the figure, the complete configuration is modeled in order to simulate flight conditions. For these computations, CFL3D is coupled to an unstructured flow solver, with CFL3D being used over the forward part of the aircraft, and the unstructured solver being used over the aft part of the aircraft.[32] The use of this hybrid approach renders the grid generation problem much simpler. The bottom part of the figure shows the results of a computation performed only on the forward portion, without coupling to the unstructured solver, simulating a wind-tunnel test. The object of this study was to investigate the control reversal (change of sign of yawing moment) that occurs for small strake deflections. Computations were performed for 0, 10, and 90 degrees of strake deflection. The predicted yawing moments are in good agreement with the wind-tunnel data.

Advanced Ducted Propeller

Figures 3 and 4 show an application of the code to a turbomachinery flow. The configuration is a wind-tunnel model of an advanced ducted propeller,[33] with 16 fan blades and 20 exit guide vanes. The rotor speed is 16,900 RPM and the Mach number is 0.2. The computations are performed time-accurately, using dynamic grids that move relative to one another across a planar interface midway between the fan blades and the exit guide vanes. Passage-averaged aerodynamic results agree well with data and results from another code.[34] The grid and time step used in this simulation are chosen to capture a particular forward-propagating duct acoustic mode that results from the highly nonlinear rotor wake-stator blade interaction. The CFL3D computation successfully generates this mode and propagates it forward of the fan face in the duct without attenuation. The inlet pressures from the computation are used as input to a linearized far-field noise-prediction code.

References

1 Van Leer, B., “Flux Vector Splitting for the Euler Equations,” *Lecture Notes in Physics*, Vol. 170, 1982, pp. 501-512.

2 Van Leer, B., “Towards the Ultimate Conservative Difference Scheme V: A Second-Order Sequel to Godunov’s Method,” *Journal of Computational Physics*, Vol. 32, 1979, pp. 101-136.

3 Godunov, S., “Finite Difference Method for Numerical Computation of Discontinuous Solutions of the Equations of Fluid Dynamics,” *Matematicheskii Sbornik*, Vol. 47, No. 3, 1959, p. 271, Cornell Aeronautical Lab (CALSPAN) translation.

[4] Thomas, J. L., van Leer, B., and Walters, R.W., “Implicit Flux-Split Schemes for the Euler Equations,” AIAA 65-1680, July 1985.

[5] Anderson, W. K., Thomas, J. L., van Leer, B., “Comparison of Finite Volume Flux Vector Splittings for the Euler Equations,” *AIAA Journal*, Vol. 24, No. 9, 1986, pp. 1453-1460.

[6] Thomas, J. L. and Walters, R. W., “Upwind Relaxation Algorithms for the Navier-Stokes Equations,” AIAA 85-1501-CP, July 1985.

[7] Newsome, R. W. and Thomas, J. L., “Computation of Leading-Edge Vortex Flows,” paper presented at the Vortex Aerodynamics Conference, NASA Langley Research Center, Hampton, VA, October 1985.

[8] Thomas, J. L. and Newsome, R. W., “Navier-Stokes Computations of Lee-Side Flows, Over Delta Wings,” *AIAA Journal*, Vol. 27, No. 12, 1989, pp. 1673-1679.

[9] Anderson, W. K., Thomas, J. L., and Whitfield, D. L., “Three-Dimensional Multigrid Algorithms for the Flux-Split Euler Equations,” NASA TP 2829, November 1988.

[10] Thomas, J. L., Krist, S. L., and Anderson, W. K., “Navier-Stokes Computations of Vortical Flows over Low-Aspect-Ratio Wings,” *AIAA Journal*, Vol. 28, No. 2, 1990, pp. 205-212.

[11] Roe, P., “Approximate Riemann Solvers, Parameter Vectors, and Difference Schemes,” *Journal of Computational Physics*, Vol. 43, 1981, pp. 357-372.

[12] Van Leer, B., Thomas, J. L., Roe, P. L., and Newsome, R. W., “A Comparison of Numerical Flux Formulas for the Euler and Navier-Stokes Equations,” AIAA 87-1104-CP, June 1987.

[13] Vatsa, V. N., Thomas, J. L., and Wedan, B. W., “Navier-Stokes Computations of a Prolate Spheroid at Angle of Attack,” *Journal of Aircraft*, Vol. 26, No. 11, 1989, pp. 986-993.

[14] Thomas, J. L., “Reynolds Number Effects on Supersonic Asymmetrical Flows over a Cone,” *Journal of Aircraft*, Vol. 30, No. 4, 1993, pp. 488-495.

[15] Thomas, J. L., “An Implicit Multigrid Scheme for Hypersonic Strong-Interaction Flowfields,” *Comm. Appl. Numerical Methods*, Vol. 8, 1992, pp. 683-693.

[16] Thomas, J. L., Rudy, D. H., Chakravarthy, S. R., and Walters, R. W., “Patched-Grid Computations of High-Speed Inlet Flows,” Symposium on Advances and Applications in CFD, Winter Annual Meeting of ASME, Chicago, IL, November 1988.

[17] Compton, W. B., III, Thomas, J. L., Abeyounis, W. K., and Mason, M. L., “Transonic Navier-Stokes Solutions of Three-Dimensional Afterbody Flows,” NASA TM 4111, July 1989.

[18] Rumsey, C. L. and Vatsa, V. N., “Comparison of the Predictive Capabilities of Several Turbulence Models,” *Journal of Aircraft*, Vol. 32, No. 3, 1995, pp. 510-514.

[19] Abid, R., Rumsey, C. L., and Gatski, T. B., “Prediction of Nonequilibrium Turbulent Flows with Explicit Algebraic Stress Models,” *AIAA Journal*, Vol. 33, No. 11, 1995, pp. 2026-2031.

[20] Rumsey, C. L., Thomas, J. L., Warren, G. P., and Liu, G. C., “Upwind Navier-Stokes Solutions for Separated Periodic Flows,” *AIAA Journal*, Vol. 25, No. 4, 1987, pp. 535-541.

[21] Rumsey, C. L., “Details of the Computed Flowfield Over a Circular Cylinder at Reynolds Number 1200,” *Journal of Fluids Engineering*, Vol. 110, December 1988, pp. 446-452.

[22] Zaman, K. B. M. Q., McKinzie, D. J., and Rumsey, C. L., “A Natural Low-Frequency Oscillation of the Flow over an Airfoil Near Stalling Conditions.” *J. Fluid Mech.*, Vol. 202, 1989, pp. 403-442.

[23] Anderson, W. K., Thomas, J. L., and Rumsey, C. L., “Extension and Application of Flux-Vector Splitting to Unsteady Calculations on Dynamic Meshes,” *AIAA Journal*, Vol. 27, No. 6, 1989, pp. 673-674; also AIAA 87-1152-CP, June 1987.

[24] Rumsey, C. L. and Anderson, W. K., “Some Numerical and Physical Aspects of Unsteady Navier-Stokes Computations Over Airfoils Using Dynamic Meshes,” AIAA 88-0329, January 1988.

[25] Rumsey, C. L. and Anderson, W. K., “Parametric Study of Grid Size, Time Step, and Turbulence Modeling on Navier-Stokes Computations Over Airfoils,” AGARD 62nd Meeting of the Fluid Dynamics Panel Symposium on Validation of CFD, AGARD CP-437, Vol. 1, 1988, pp. 5-1 - 5-19.

[26] Rumsey, C., Sanetrik, M., Biedron, R., Melson, N., and Parlette, E., "Efficiency and Accuracy of Time-Accurate Turbulent Navier-Stokes Computations," *Computers and Fluids*, Vol. 25, No. 2, 1996, pp. 217-236.

[27] Biedron, R. T. and Thomas, J. L., "A Generalized Patched-Grid Algorithm with Application to the F-18 Forebody with Actuated Control Strake," *Computing Systems in Engineering*, Vol. 1, Nos. 2-4, 1990, pp. 563-576.

[28] Rumsey, C., "Computation of Acoustic Waves Through Sliding-Zone Interfaces," *AIAA Journal*, Vol. 35, No. 2, 1997, pp. 263-268.

[29] Krist, S. L., "A Grid-Overlapping Technique Applied to a Delta Wing in a Wind Tunnel," Masters Thesis, George Washington University, January 1994.

[30] Krist, S. L., Thomas, J. L., Sellers, W. L., III, and Kjelgaard, S. O., "An Embedded Grid Formulation Applied to a Delta Wing," AIAA 90-0429, January 1990.

[31] Jones, K. M., Biedron, R. T., and Whitlock, M., "Application of a Navier-Stokes Solver to the Analysis of Multi-element Airfoils and Wings Using Multizonal Grid Techniques," AIAA 95-1855, June 1995.

[32] Biedron, R. T., "Comparison of ANSER Control Device Predictions with HARV Flight Tests," Proceedings of the NASA High-Angle-of-Attack Technology Conference, 1997. To appear as a NASA CP.

[33] Thomas, R. H., Gerhold, C. H., Farassat, F., Santa Maria, O. L., Nuckolls, W. E., DeVilbiss, D. W., "Far Field Noise of the 12 Inch Advanced Ducted Propeller Simulator," AIAA 95-0722, January 1995.

[34] Adamczyk, J. J., Celestina, M. L., Beach, T. A., Barnett, M., "Simulation of Three-Dimensional Viscous Flow Within a Multistage Turbine," *ASME Journal of Turbomachinery*, Vol. 112, July 1990, pp. 370-376.

Figures

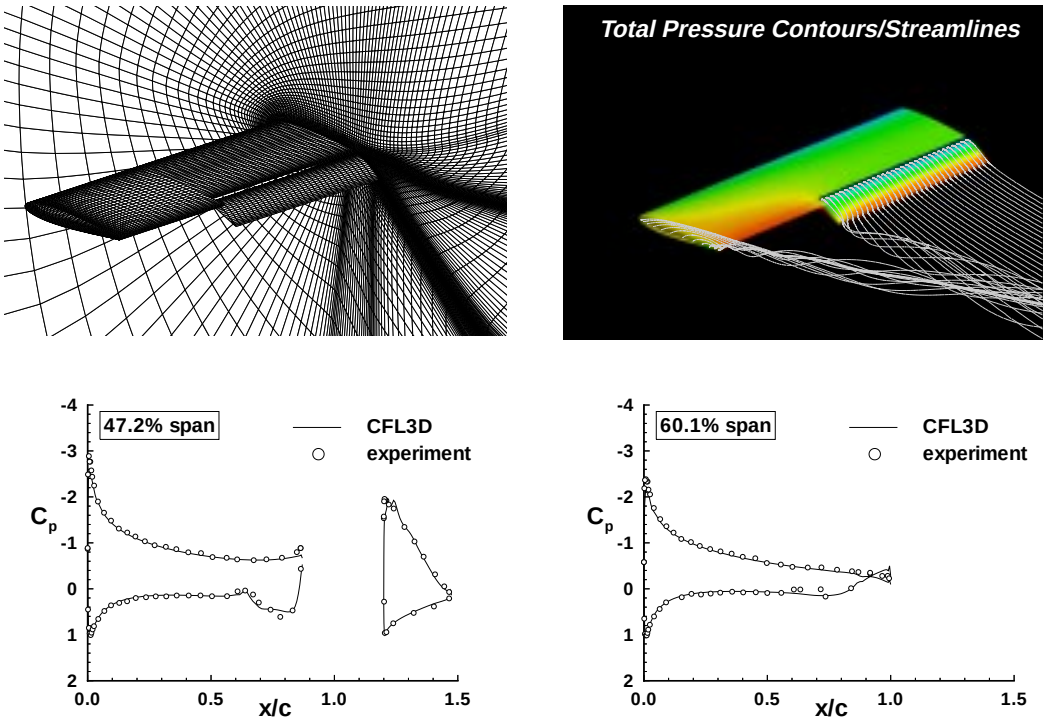

Figure 1: Flow past a wing with a partial-span flap. The Reynolds number is 3.3 million, the Mach number is 0.15, the angle of attack is 4 degrees, and the flap deflection is 30 degrees. Shown are the grid, computed total pressure contours and streamlines, as well as comparison of computed surface pressures with wind-tunnel data.

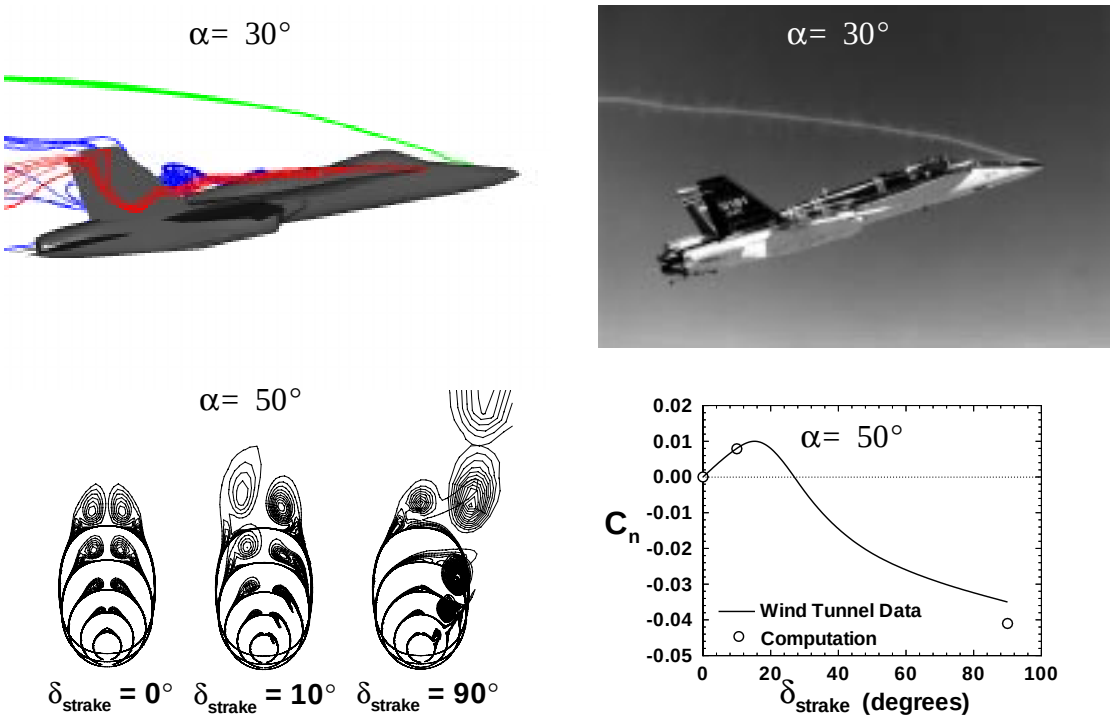

Figure 2: High-angle-of-attack control strake for the F/A-18. The top pair of images shows the comparison of the computed strake vortex and in-flight flow visualization. The bottom pair of images shows a computation illustrating control reversal at low strake deflections, with comparison to yawing-moment data from wind-tunnel tests.

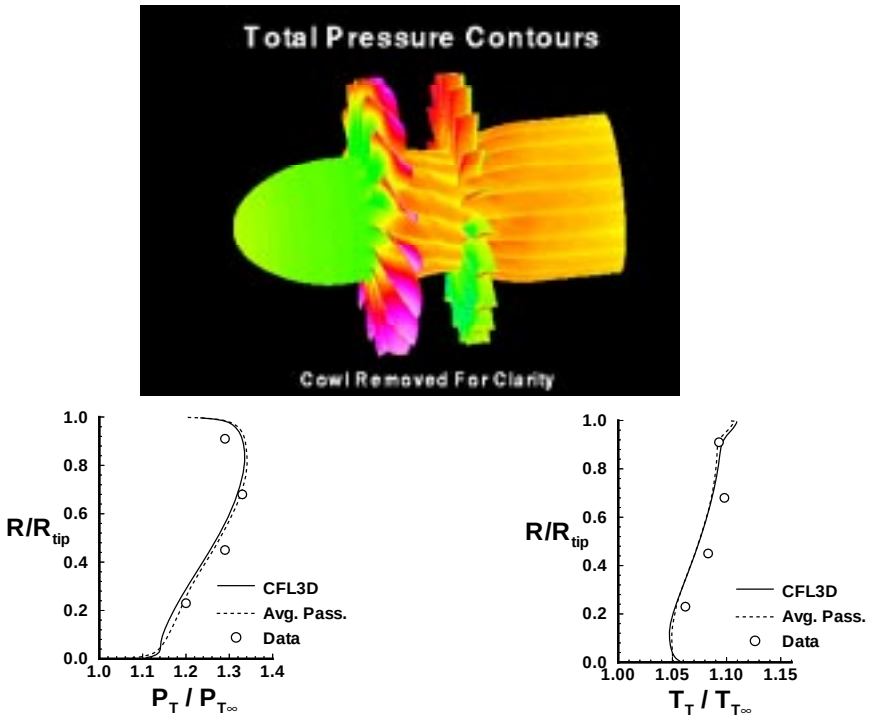

Figure 3: Flow through an ADP model with 16 rotor blades and 20 exit guide vanes. The rotor speed is 16,900 rpm, and the Mach number is 0.2. Shown are total pressure contours, as well as comparison of the passage-averaged CFL3D computation with experimental data and a computation using the average passage equations.

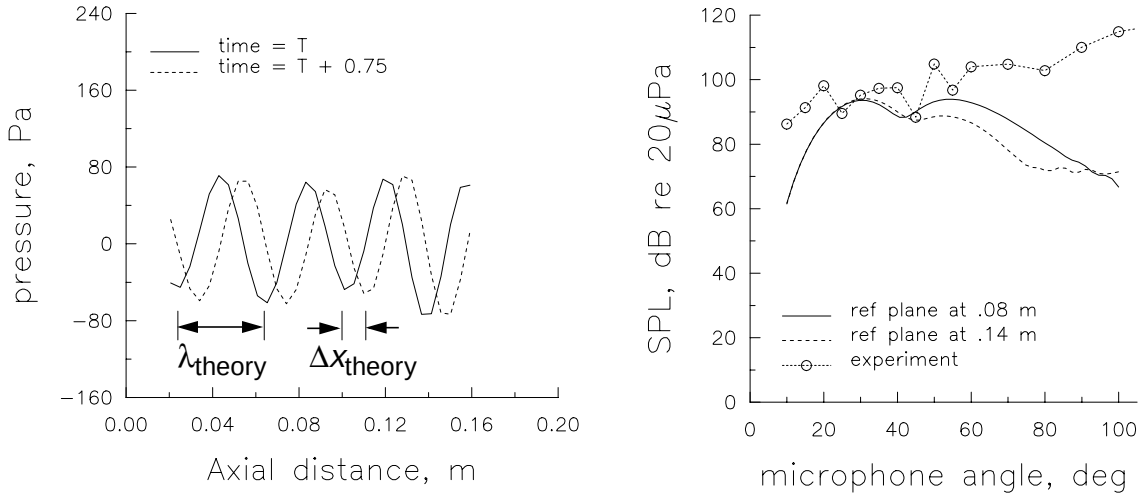

Figure 4: Flow through an ADP model with 16 rotor blades and 20 exit guide vanes. The left figure shows the real part of the magnitude of the (-4,1) duct acoustic mode at two instants in time, in comparison with infinite duct theory. The right figure shows the far field sound pressure levels due to all the radial orders of the (-4,n) modes as a function of microphone angle, using two different reference planes inside the duct. The left-hand lobe, which is insensitive to reference plane position, is due primarily to the (-4,1) mode. High experimental noise levels at the largest microphone angles are due to contamination from aft-end noise.